Supporting Information

Modulating the crystalline assembly of paramagnetic Au_{25} nanoclusters by external magnetic field

Zhipeng Chen,† Xinran Xu,† Yajie Guan, Nan Xia*

Key Laboratory of Functional Molecular Solids, Ministry of Education, College of Chemistry and Materials Science, Anhui Normal University, Wuhu 241000, P.R. China
E-mail: xianan@ahnu.edu.cn

1. Methods

Materials. All chemicals used are commercially available and were used without any additional purification steps. Tetrachloroauric (III) acid ($HAuCl_4 \cdot 4H_2O$, 99.7%), tetraoctylammonium bromide (TOAB, 98.0%), 2-phenylethanethiol (PET, 97.0%), sodium borohydride ($NaBH_4$, 98.0%) was purchased from Aladdin. Methanol (99.5%), dichloromethane (AR), petroleum ether (AR), toluene (99.5%), acetonitrile (99.0%), hydrogen peroxide (H_2O_2, 30%) was purchased from Sinopharm chemical reagent co., ltd.

Synthesis of neutral Au_{25} nanoclusters. The Au_{25} anions were first prepared according to the previous literature.[1] Then, 50 mg crystals of Au_{25} anions were dissolved in 20 ml dichloromethane and treated with 1 ml H_2O_2 (30%). After stirring at room temperature for 1 h, the organic solution was extracted and purified using preparative thin-layer chromatography (dichloromethane/petroleum ether: 1/1) to obtain Au_{25}^0 nanoclusters.

Crystal growth and transformation of neutral Au_{25} nanoclusters. Au_{25}^0 were crystallized in a mixed solvent of 200 μl toluene and 360 μl ethanol for 2~3 days. Au_{25}^0–T crystals were obtained by treating Au_{25}^0 crystals in the mother liquor at 50 °C for 60 h. Au_{25}^0 crystals can be transformed to Au_{25}^0–TM crystals at 50 °C using neodymium magnet. The magnetic intensity was measured by a DLX-STW1045 teslameter.

Characterization. Optical absorption spectra were acquired in the range of 190−1000 nm using a Metash UV-6100A spectrophotometer. The single crystal X-ray diffraction data was collected on a Bruker D8 Venture X-ray diffractometer (Bruker, Germany). X-band CW-EPR spectra were collected using a Bruker EMX plus 10/12 X-band EPR spectrometer equipped with an ER4119HS (TE011) high-Q cavity at 2 K. Cryogenic temperatures were achieved using an Oxford Instruments ESR910 liquid helium flow cryostat and an Oxford Instruments ITC503 temperature controller. For the rotating EPR measurement, a piece of dark plate-shaped crystal with dimensions ~1.0*1.0*0.4 mm was mounted onto the sample holder using high vacuum grease. The crystal was

embedded in the grease for immobilization during testing. A programmable one-axis goniometer was used for the sample rotation with angle step of 10°.

2. Figures and Tables

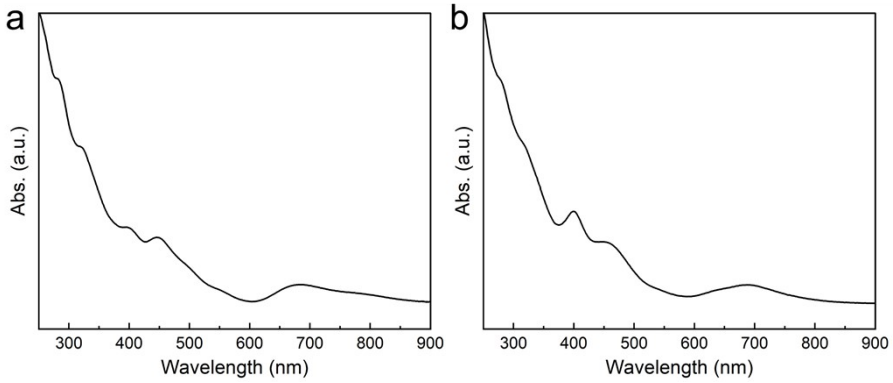

Figure S1. Typical UV/vis/NIR spectra of (a) Au_{25} anions and (b) Au_{25}^0.

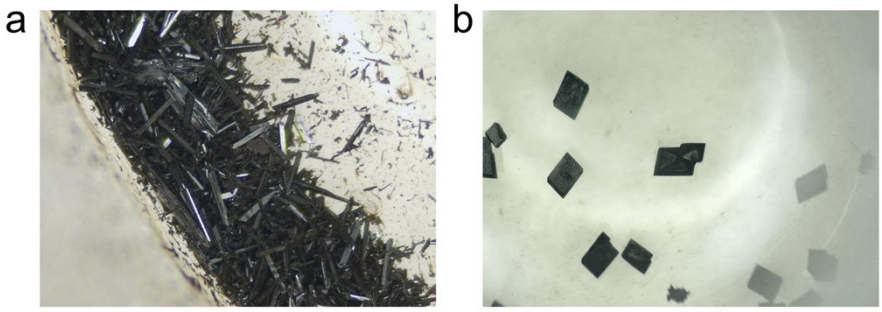

Figure S2. Optical microscopy image of (a) needle-like crystals of Au_{25} anions and (b) block crystals of Au_{25}^0.

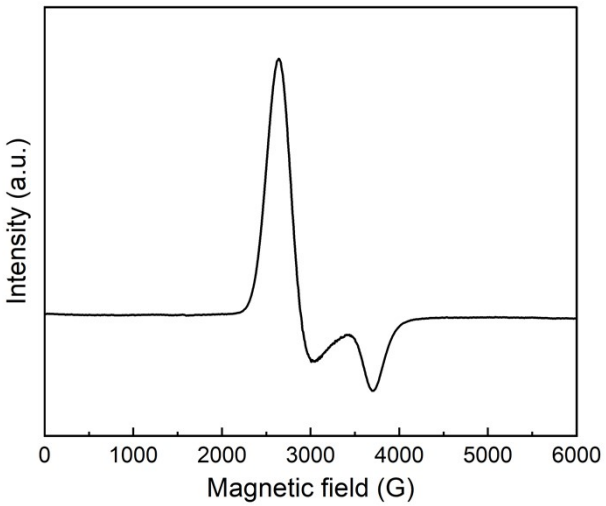

Figure S3. Typical EPR signal of Au_{25}^0 in dichloromethane at 2 K.

Table S1. Cell parameters of Au_{25}^0–TM crystals under different magnetic intensities.

	50°C + 60 mT	50°C + 120 mT	50°C + 180 mT	50°C + 280 mT
Unit cell dimensions	a = 16.13Å	a = 16.13Å	a = 16.19Å	a = 16.17Å
	b = 17.75Å	b = 17.76Å	b = 17.83Å	b = 17.78Å
	c = 17.95Å	c = 17.97Å	c = 18.11Å	c = 17.97Å
	α = 65.01°	α = 65.00°	α = 64.90°	α = 64.94°
	β = 64.54°	β = 64.58°	β = 64.50°	β = 64.56°
	γ = 81.14°	γ = 81.15°	γ = 81.12°	γ = 81.14°

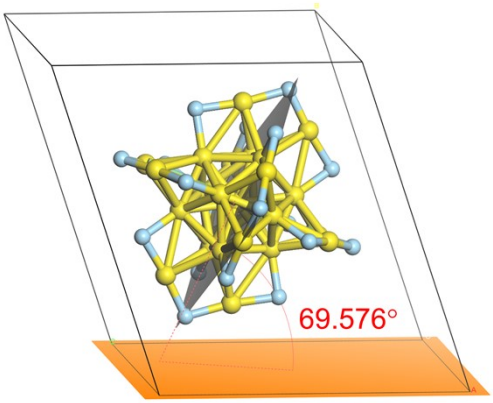

Figure S4. The orientation of Au_{25}^0 NC in the lattice.

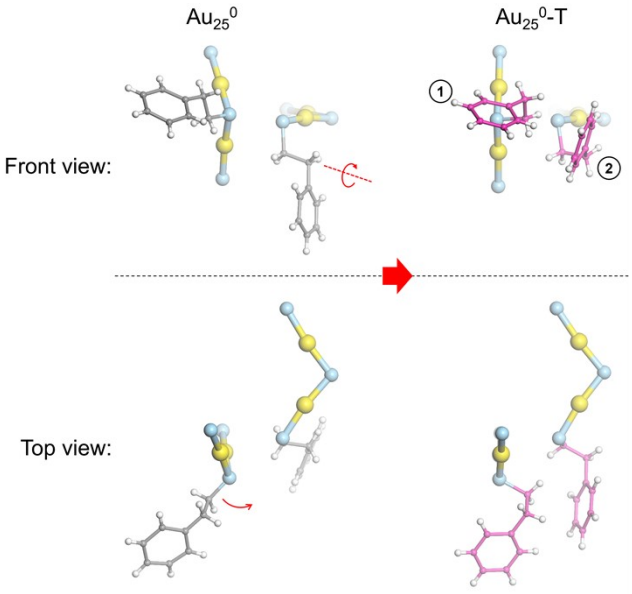

Figure S5. Detailed conformational changes of the ligands between Au_{25}^0 and Au_{25}^0–T.

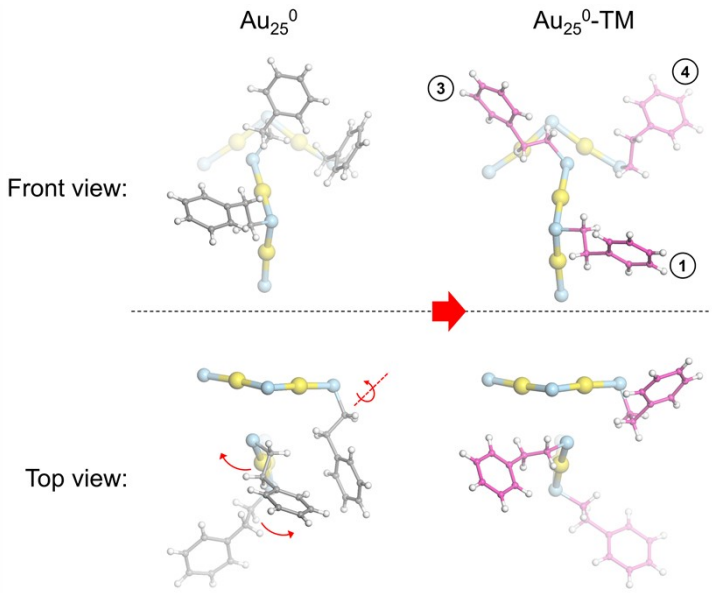

Figure S6. Detailed conformational changes of the ligands between Au_{25}^0 and Au_{25}^0–TM.

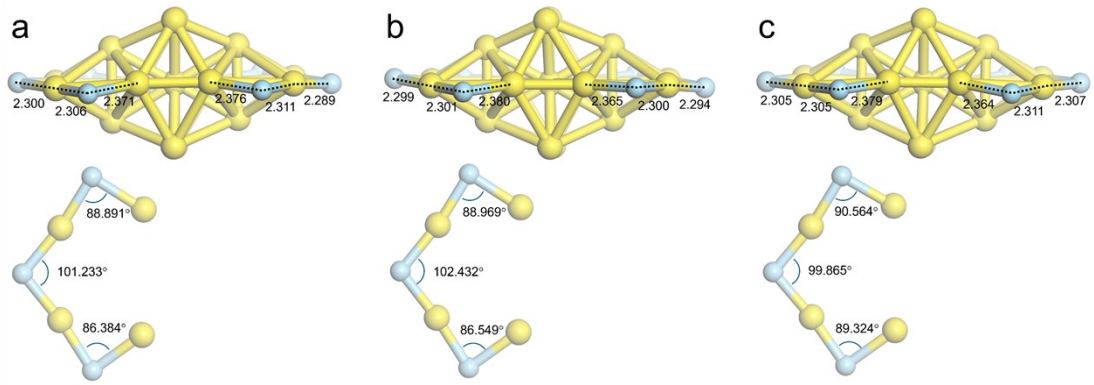

Figure S7. Comparison of the Au–S bond (unit of Å) and Au–S–Au angle of the staples in (a) Au_{25}^0, (b) Au_{25}^0–T, and (c) Au_{25}^0–TM along x axis.

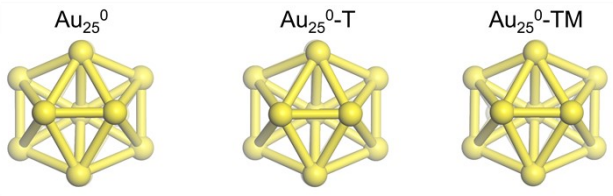

Au_{25}^0	Au_{25}^0-T	Au_{25}^0-TM
Au···Au distance	Au···Au distance	Au···Au distance
5.598	5.598	5.621
5.567	5.602	5.591
5.582	5.568	5.602
5.549	5.538	5.552
5.550	5.572	5.564
5.617	5.582	5.589

Figure S8. Size comparison of the Au_{13} kernel in Au_{25}^0, Au_{25}^0–T, and Au_{25}^0–TM.

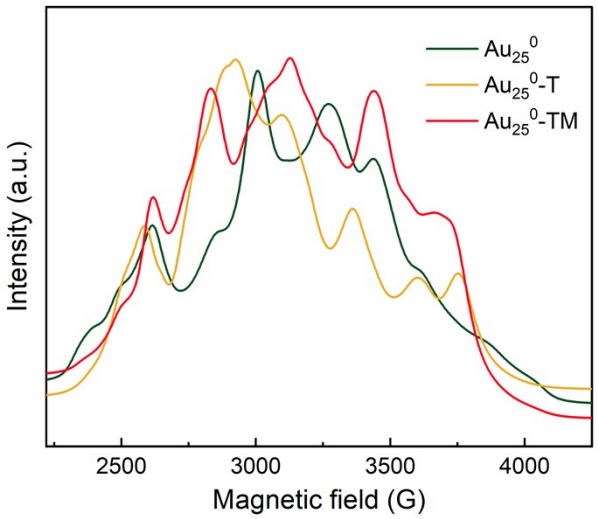

Figure S9. The integrated EPR peaks for Au_{25}^0, Au_{25}^0–T, and Au_{25}^0–TM microcrystals.

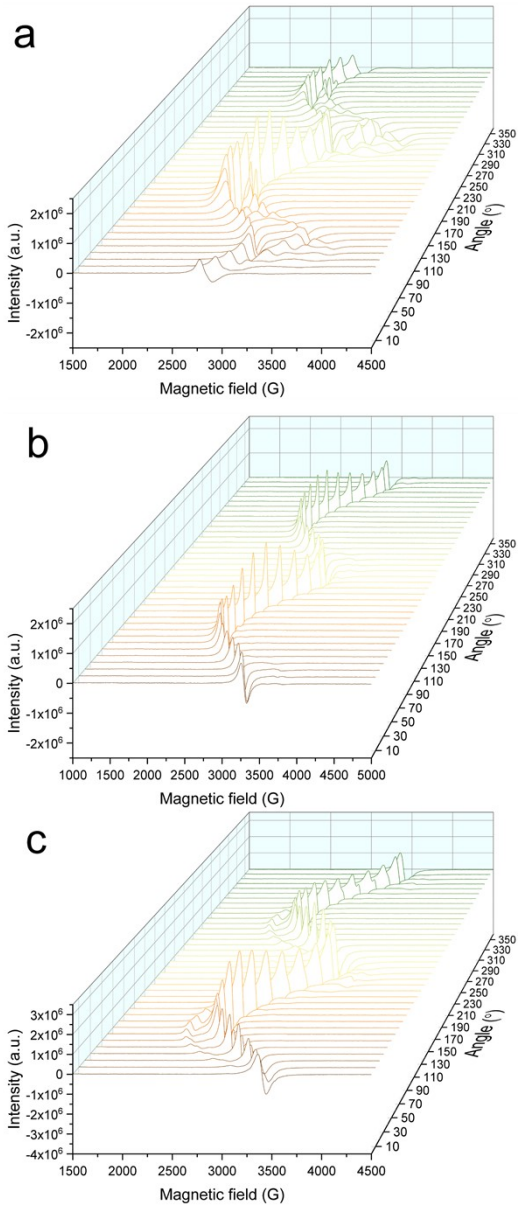

Figure S10. Angle-dependent EPR spectra of (a) Au_{25}^0, (b) Au_{25}^0–T, and (c) Au_{25}^0–TM single crystals.

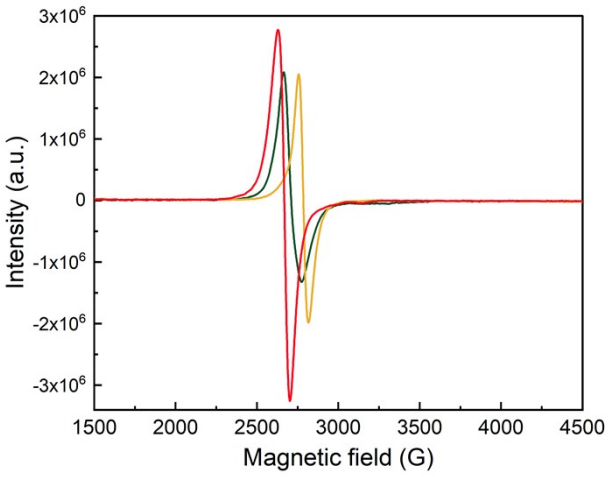

Figure S11. The comparison of maximum EPR peaks for Au_{25}^{0}, Au_{25}^{0}–T, and Au_{25}^{0}–TM single crystals.

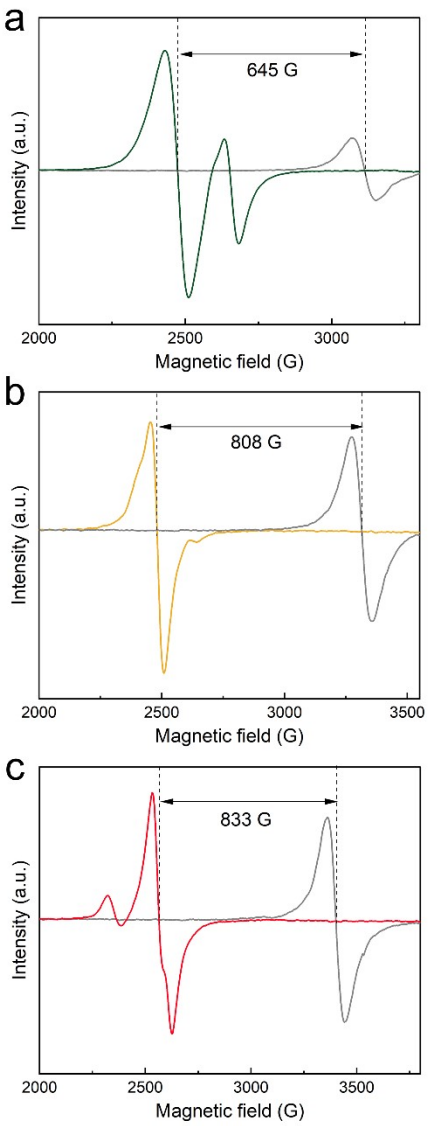

Figure S12. The largest H_r shift of (a) Au_{25}^{0}, (b) Au_{25}^{0}–T, and (c) Au_{25}^{0}–TM single crystals during rotational EPR experiments.

Table S2. Crystal data and structure refinement for Au_{25}^0.

Identification code	mo_20250224_ZhWZ_1_0m
Empirical formula	$C_{144}H_{162}Au_{25}S_{18}$
Formula weight	7393.97
Temperature/K	213.00
Crystal system	monoclinic
Space group	$P\,2_1/c$
a /Å	17.3927(6)
b /Å	27.6592(9)
c /Å	18.4466(7)
α /°	90
β /°	111.4700(10)
γ /°	90
Volume /Å^3	8258.3(5)
Z	2
ρ_{calc} g/cm^3	2.973
μ /mm^{-1}	22.373
F(000)	6578.0
Radiation	MoKα (λ = 0.71073)
2θ range for data collection /°	4.302 to 54.998
Index ranges	$-22 \le h \le 22$, $-35 \le k \le 35$, $-23 \le l \le 21$
Reflections collected	110450
Independent reflections	18916 [R_{int} = 0.0832, R_{sigma} = 0.0592]
Data/restraints/parameters	18916/821/1088
Goodness-of-fit on F^2	1.035
Final R indexes [I>=2σ (I)]	R_1 = 0.0345, wR_2 = 0.0697
Final R indexes [all data]	R_1 = 0.0531, wR_2 = 0.0767
Largest diff. peak/hole / eÅ^{-3}	2.02/–1.45

Table S3. Crystal data and structure refinement for Au_{25}^{0}–T.

Identification code	cu_250222WQANGZ_AU3_0m
Empirical formula	$C_{144.25}H_{162.5}Au_{25}Cl_{0.5}S_{18}$
Formula weight	7415.20
Temperature/K	213.00
Crystal system	orthorhombic
Space group	*P* c c n
a /Å	27.1121(12)
b /Å	31.5764(12)
c /Å	18.6459(8)
α /°	90
β /°	90
γ /°	90
Volume /Å^3	15962.8(12)
Z	4
ρ_{calc} g/cm^3	3.085
μ /mm^{-1}	44.557
F(000)	13198.0
Radiation	CuKα (λ = 1.54184)
2θ range for data collection /°	4.296 to 136.71
Index ranges	$-30 \le h \le 32$, $-38 \le k \le 36$, $-22 \le l \le 21$
Reflections collected	136324
Independent reflections	14588 [R_{int} = 0.0825, R_{sigma} = 0.0392]
Data/restraints/parameters	14588/194/901
Goodness-of-fit on F^2	1.068
Final R indexes [I>=2σ (I)]	R_1 = 0.0363, wR_2 = 0.0889
Final R indexes [all data]	R_1 = 0.0415, wR_2 = 0.0917
Largest diff. peak/hole / eÅ^{-3}	2.05/–1.79

Table S4. Crystal data and structure refinement for Au_{25}^{0}–TM.

Identification code	mo_250222WQANGZ_AU4_0m
Empirical formula	$C_{158}H_{178}Au_{25}S_{18}$
Formula weight	7578.24
Temperature/K	213.00
Crystal system	triclinic
Space group	$P\,\bar{1}$
a /Å	16.1923(8)
b /Å	17.8281(10)
c /Å	18.1066(10)
α /°	64.902(2)
β /°	64.499(2)
γ /°	81.122(2)
Volume /Å^3	4269.8(4)
Z	1
ρ_{calc} g/cm^3	2.947
μ /mm^{-1}	21.641
F(000)	3389.0
Radiation	MoKα (λ = 0.71073)
2θ range for data collection /°	4.392 to 52
Index ranges	$-19 \le h \le 19$, $-21 \le k \le 21$, $-22 \le l \le 22$
Reflections collected	82750
Independent reflections	16750 [R_{int} = 0.0800, R_{sigma} = 0.0614]
Data/restraints/parameters	16750/210/972
Goodness-of-fit on F^2	0.971
Final R indexes [I>=2σ (I)]	R_1 = 0.0359, wR_2 = 0.0843
Final R indexes [all data]	R_1 = 0.0485, wR_2 = 0.0911
Largest diff. peak/hole / eÅ^{-3}	1.56/–1.98